Journal of the Meteorological Society of Japan, Vol. 90, No. 2, pp. 235–254, 2012
DOI:10.2151/jmsj.2012-206

Improved Performance of Simulated Japanese Climate with a Multi-Model Ensemble

Noriko N. ISHIZAKI, Izuru TAKAYABU

Meteorological Research Institute, Tsukuba, Japan

Mitsuo OH'IZUMI

Meteorological College, Kashiwa, Japan

Hidetaka SASAKI

Meteorological Research Institute, Tsukuba, Japan

Koji DAIRAKU, Satoshi IIZUKA

National Research Institute for Earth Science and Disaster Prevention, Tsukuba, Japan

Fujio KIMURA

Research Institute for Global Change, Japan Agency for Marine-Earth Science and Technology, Yokohama, Japan

Hiroyuki KUSAKA

Center for Computational Sciences, University of Tsukuba, Tsukuba, Japan

Sachiho A. ADACHI

Research Institute for Global Change, Japan Agency for Marine-Earth Science and Technology, Yokohama, Japan

Kazuo KURIHARA, Kazuyo MURAZAKI

Meteorological Research Institute, Tsukuba, Japan

and

Kenji TANAKA

Disaster Prevention Research Institute, Kyoto University, Kyoto, Japan

(Manuscript received 27 December 2010, in final form 4 January 2012)

Abstract

This paper analyzed the downscaling products for Japanese climate using five regional climate models (RCMs) with horizontal meshsize of 20 km with boundary conditions given from JRA-25 reanalysis. The RCMs successfully reproduced the temporal variations and geographic distribution of temperature and precipitation. Skill scores for the surface temperature were improved by the downscaling. The JRA-25 underestimated the precipitation amount for summer and winter seasons, and the RCMs reduced the error, especially in winter. The RCMs showed common features, such as a warm bias in the areas with a monthly-mean temperature lower than the freezing point, an overestimation of weak rainy days, and an underestimation of heavy rainy days. The comparison among five RCMs suggests that the warm bias is due to the lack of model resolution and the precipitation bias is related to the convective parameterization. The multi-RCM ensemble mean has considerable advantages over the individual RCM in regards to the bias and skill scores of surface temperature and precipitation, although it still showed the warm bias in snow areas in winter. The data set of the multi-model dynamical downscaling is expected to contribute to impact studies on the forthcoming climate change in Japan.

1. Introduction

Climate change, particularly global warming, has been attracting enormous attention worldwide because a warmer climate may have a serious impact on our lives ecological systems. To assess the impact of climate change and develop effective measures to mitigate its effects, spatially detailed and accurate climate projection is required. Recently, high resolution general circulation models (GCMs; Yukimoto et al. 2006; Satoh et al. 2008; Sakamoto et al. 2011) have been developed. However, they inevitably require a computational burden for long-term integration. The dynamical downscaling (DDS) method, using regional climate models (RCMs), can provide fine-grid physically-consistent data for a particular domain from coarse-grid information as the GCM. Many papers have demonstrated the availability of RCMs to improve simulations and our understanding (e.g., Giorgi and Bates 1989; Giorgi 1990; Leung and Ghan 1995; Mearns et al. 1995; Yoshikane et al. 2001; Kunkel et al. 2002; Wang et al. 2003; Sen et al. 2004; Feser and von Storch 2008; Ishizaki and Takayabu 2009). In Giorgi and Bates (1989) and Giorgi (1990), first month-long nested simulations without any reinitialization, along with the RCM, added fine structure to the precipitation and temperature distribution to the large-scale circulation, followed by the external forcing of a GCM. Leung and Ghan (1995) successfully simulated realistic orographic precipitation in a RCM with a state-of-the-art subgrid-scale parameterization on topographic elevation. Kunkel et al. (2002) effectively simulated the seasonal march of heavy rainfall events across the United States. Feser and von Storch (2008) realistically simulated typhoons in Southeast Asia from the view point of core pressure and wind speed. By performing several sensitivity experiments using RCM, Yoshikane et al. (2001) and Yoshikane and Kimura (2003) showed the formation mechanisms of the Baiu front and south Pacific convergence zone. Ishizaki and Takayabu (2009) explained three different heating mechanisms for warming events on the lee side using trajectory analysis in RCM simulations. At present, the RCM is recognized as a powerful tool to zoom in for a closer look at regional climate.

Corresponding author and present affiliation: Noriko N. Ishizaki, Japan Agency for Marine-Earth Science and Technology, 3173-25 Showa-machi, Kanazawa-ku, Yokohama, Kanagawa 236-0001, Japan
E-mail: nishizak@jamstec.go.jp
©2012, Meteorological Society of Japan

On the other hand, we notice that the RCM outputs include biases and uncertainties (e.g., Giorgi and Francisco 2000; Christensen et al. 2001). If one used a single model result, one could not estimate a systematic error depending on the RCM. The RCM inter-comparison is then needed to address the model bias problem. This underlies the motivation of multi-RCM ensemble studies (Rummukainen 2009), though it has suffered from a large uncertainty that is attributed to the choice of a GCM as the lateral boundary condition of the RCM simulations (e.g., Rowell 2006; Deque et al. 2007). The DDS with reanalysis data, not GCM outputs, is just a hindcast RCM simulation under the background state without any biases. The multi-RCM comparison of this kind of simulation then extracts the performance and characteristics of the RCMs.

Recently, several projects performing inter-comparisons of RCMs have been launched in many developed countries: CORDEX (Giorgi et al. 2009), ENSEMBLES (Christensen et al. 2009), PRUDENCE (Jacob et al. 2007), NARCCAP (Wang et al. 2009), RMIP (Fu et al. 2005), and CaRD10 (Kanamitsu and Kanamaru 2007). Jacob et al. (2007) indicated that the high pressure bias over the Mediterranean region was accompanied with a warm, wet bias in Northern Europe and a cold, dry bias in Southern Europe during the winter season. They suggested that the reproducibility of the frequency of the blocking event in a GCM affected the performance of the inter-annual variability of European climate in a nested RCM. Wang et al. (2009) examined how accurately RCMs simulated seasonal and interannual variability in precipitation along the intermountain region of the western United States using six models. They showed that RCMs clearly improved the seasonal cycle of precipitation. They moreover suggested that a false ENSO signal led to precipitation bias in the western United States. In contrast with the large impact of extratropical stationary waves on the European and North American climate, the Asian climate is generally controlled by the monsoon. The subtropical anticyclone and the Okhotsk high add a complexity to the Northeast Asian summer climate. RCMs produced diverse features in the precipitation bias in the Asian monsoon region (Fu et al. 2005). Takayabu et al. (2007) indicated that the model diversity and the model bias were less in higher latitudes, even in the monsoon region. However, the cause of RCM bias and the advantage of using multi-RCM in the vicinity of Japan have not been adequately discussed so far.

The purpose of this study is to assess the characteristics and capability of RCMs around Japan by per-

Table 1. Designs of RCMs. The K-F and A-S denote Kain-Fritsch scheme (Kain and Fritsch 1993) and Arakawa-Schubert scheme (Arakawa and Schubert 1974), respectively.

	MRI NHRCM	NIED RAMS	TSKB RAMS	TSKB WRF	MRI RCM20
Dynamical basis	Non-hydrostatic				hydrostatic
Horizontal meshsize	20 km				
Grids	171 × 161 × 40	128 × 144 × 27	130 × 140 × 30	130 × 140 × 31	181 × 181 × 36
Land scheme	MJ-SiB	LEAF2+GEMTM	BATS	Noah LSM	QL-SVATS
Convective scheme	K-F	K-F	A-S	K-F	A-S
Nudging system	No	No	No	No	Spectral boudary coupling method (Kida et al. 1991)
References	Saito et al. 2006	Pielke et al. 1992	Adachi et al. 2009	Skamarock et al. 2008	Kurihara et al. 2005

forming hindcast experiments with five state-of-the-art RCMs with horizontal meshsize of 20 km. There are three reasons why we focus on the Japanese region. First, a surface observation network, with one station per about 300 km^2, has been operated by Japan Meteorological Agency (JMA) for more than 30 years. The RCMs with a 20-km meshsize can provide data that are reasonably validated with the surface observation. Second, the RCM calculation for the Japanese territory may save computational cost, and we are then able to perform long-term integration with the multiple RCMs. Finally, Japan has a variety of climates in its meridionally elongated archipelago in the mid-latitudes. The hindcast DDS for the Japanese territory may reveal model performance from tropical to sub-arctic climates. The rest of this paper is organized as follows. Models and data are described in Section 2, and biases and a skill score for each RCM are presented in Section 3. We discuss the cause of the common biases in RCMs and key agents to improve the model in Section 4. Finally, the conclusions are presented in Section 5.

2. Models and data

2.1 Models and experiment

Here we perform hindcast DDS (Type 2 of DDS categories proposed by Castro et al. 2005) following unique protocol by using five RCMs; MRI-NHRCM, NIED-RAMS, TSKB-RAMS, TSKB-WRF and MRI-RCM20[1] (Table 1). The protocol specified the model domain, including the Japanese territory (Fig. 1), even though the calculation domain, the lateral buffer zone, and the surface height are not exactly the same as the RCMs. Note that Japan contains meridionally elongated archipelago and complex topography within a small land mass that brings a variety of climates (e.g., Ishizaki and Takayabu 2009). RCMs are nested in the Japanese reanalysis JRA-25 with the grid interval of 1.25° × 1.25°, in which the typhoon bogus was embedded (Onogi et al. 2007). Sea surface temperatures (SSTs) are also taken from the reanalysis. The horizontal meshsize is commonly set to 20 km and the number of vertical levels is enough to resolve boundary layer processes. The numerical experiment is conducted for the 20-year period from 1985 to 2004.

The dynamical core is based on hydrostaticity in RCM20, and non-hydrostatic formulation in four additional models. The model is forced by external large-scale flow through the lateral boundary, except for RCM20 with spectral nudging (Kida et al. 1991). The Kain-Fritsch convective parameterization (Kain and Fritsch 1993) is implemented in NHRCM, NRAMS and TWRF, while other two RCMs use the Arakawa-Schubert scheme (Arakawa and Schubert 1974) for calculating convective precipitation. The land surface schemes consist of MRI/JMA simple biosphere model (MJ-SiB; Hirai et al. 2007) for NHRCM, the land-ecosystem atmosphere feedback model (LEAF2; Walko et al. 2000) and general energy and mass transfer model (GEMTM; Eastman et al. 2001) for NRAMS, the biosphere-atmosphere transfer scheme (BATS; Dickinson et al. 1993) for TRAMS, the Noah land surface model (LSM; Ek et al. 2003) for TWRF, and the soil-vegetation-atmosphere transfer scheme (QL-SVATS; Murazaki et al. 2005) for RCM20, respectively.

[1]The JMA developed NHRCM, a derivative of its operational weather forecast model (Saito et al. 2006) and RCM20 (Kurihara et al. 2005). NRAMS and TRAMS, both based on regional atmospheric modeling system (RAMS; Pielke et al. 1992), were developed in the National Research Institute for Earth Science and Disaster Prevention (NIED) and University of Tsukuba, respectively. TWRF is based on the advanced research version of weather research and forecasting model (WRF-ARW; Skamarock et al. 2008).

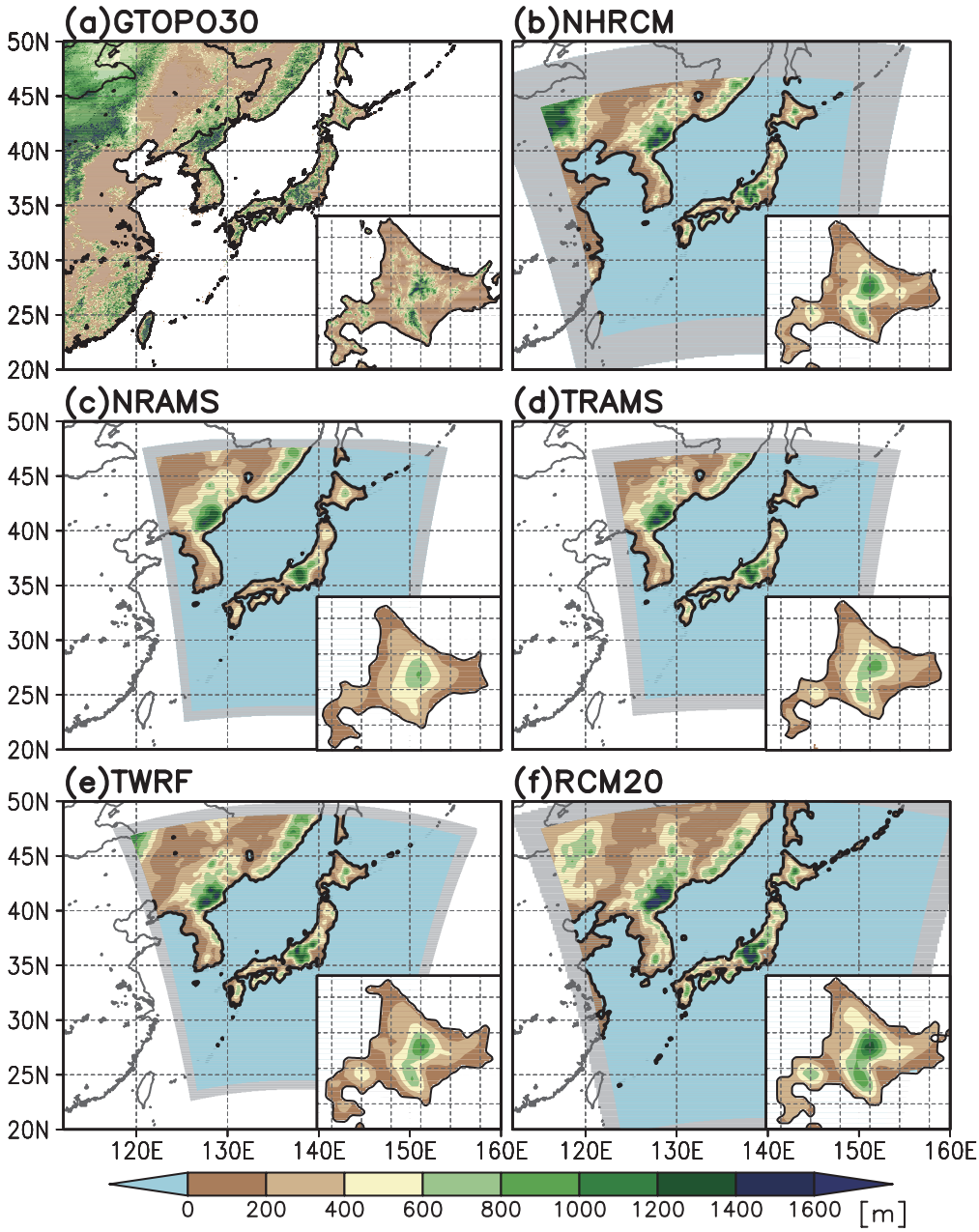

Fig. 1. (a) Surface height based on GTOPO30. (b–f) The nested domains and surface height (m) for (b) NHRCM, (c) NRAMS, (d) TRAMS, (e) TWRF, and (f) RCM20. Gray shading denotes the lateral buffer zones. The close-up figures for the Hokkaido region are also shown in the bottom right corner of each panel.

2.2 *Data*

We use surface air temperature and precipitation data for Japan called Automated Meteorological Data Acquisition System (AMeDAS) and Meshed Climatological dataset (Shimazu et al. 2003) to evaluate the RCMs' outputs. The AMeDAS stations were uniformly installed over the land surface in the Japanese territory, and have been operated by the JMA to observe temper-

ature, wind, sunshine duration, and precipitation. The average distance between adjacent stations is 17 km. The Meshed Climatological data are estimated from surface observations, including AMeDAS, using multiple regressions based on geographical and urban factors with 1 km × 1 km grid across Japan. APHRO_JP (Kamiguchi et al. 2010), a gridded daily precipitation dataset, is essentially based on the AMeDAS observation and assisted in our analysis.

2.3 *Bias detection method*

The model results are compared with Meshed Climatological data at a grid spacing of 0.2° × 0.2°. A bias detection tool (Tanaka et al. 2008), based on the regional mean values for 60 Japanese provinces, is used (Appendix). Since the RCM gridmesh is as dense as the AMeDAS observation network, AMeDAS stations can be found near most of the model grids. The "true" value at a model grid is regarded as the mean for its neighboring stations where the distance from it is less than model grid spacing. This process is applied for surface temperature after the lapse-late adjustment with 6.5 K km^{-1}, excluded are the model grids with no surrounding stations, particularly those found in mountain ranges. A monthly-mean bias can be identified as the monthly-mean model output and the monthly-mean true value. The bias detection tool takes a regional average of the bias for the Japanese province. As the "true" value is based on the AMeDAS observation, we can formally estimate the bias of analysis data. Hereafter, the bias of JRA-25 means the difference between observed values and JRA-25 reanalysis values.

3. Results

To examine how well each RCM can simulate the climatology, the differences in surface temperature between RCMs and the meshed observation data-set are shown in Fig. 2 for June–July–August and December–January–February. The RCMs, driven by JRA-25, successfully simulated the surface air temperature during summer because its bias ranged in ±1 K and is independent of topography (Figs. 2c–g). Two models gave a systematic warm bias over Japan (Figs. 2c, e), while the two other models made a systematic negative bias (Figs. 2d, g). Even though the systematic large-scale temperature bias is likely to stem from a geographical bias in the upper troposphere, the summer temperature bias for the ensemble average (Fig. 2h) is much smaller than that for JRA-25 (Fig. 2b). The winter temperatures generally had a larger bias than the summer temperatures. Four RCMs showed a warm bias over Hokkaido; two models featured a systematic warm bias briefly over Japan (Figs. 2k, l), while two other models featured a systematic cold bias in eastern Japan (Figs. 2m, n). The resultant ensemble-mean (Fig. 2p) has a better performance than JRA-25 (Fig. 2j), but the temperature bias still exceeds 1 K in Hokkaido. NHRCM and NRAMS have brief positive bias over Japan, while TRAMS and TWRF have negative bias in eastern Japan during the winter.

Japan has heavy precipitation over southern Japan during the summer season (Fig. 3a), which is largely underestimated by JRA-25 (Fig. 3b). The RCMs basically improved the precipitation bias of JRA-25, while two models have rather wet biases over Japan (Figs. 3e, f). There is a slight difference in the large-scale circulation between RCMs and JRA-25, as indicated by the sea level pressure. During winter, the precipitation pattern makes a remarkable contrast with the abundant rainfall at the Japan Sea side associated with the winter monsoon flow. The RCMs have dry bias in the rainy areas and wet bias in drier areas, which results in obscured rainfall contrast in comparison with those observed. It is likely to be associated with the weakened meridional gradient sea level pressure between the Asian continent and Japan, which is directly related to the intensity of the winter monsoon flow. The multi-model ensemble mean cannot yield an improved performance in precipitation for both seasons because the RCMs tend to show similar bias distributions, while the bias of the ensemble mean is slightly decreased as a whole.

We analyze the RCM performance based on root mean square error (RMSE) and skill scores following Taylor (2001). Note that the skill score for a single member is defined as

$$S = \frac{(1+R)^4}{4\left(\sigma + \frac{1}{\sigma}\right)^2}, \tag{1}$$

where R is the spatial correlation coefficient and σ is the standard deviation normalized by the reference spatial pattern, and that all the model data are rearranged to fit the common grid system of 0.2° in longitude by 0.2° in latitude over Japan. The traditional bias evaluation with RMSE supplements the Taylor diagram. The skill score of the surface temperature is close to agreement because it has a very high spatial correlation with the reference pattern (Fig. 4a), though the RMSE is remarkably large, especially in winter due to a systematic offset of temperature over Japan (Fig. 4b). The summer temperature in most RCMs provided a uniform bias in Japan, but that in JRA-25 provided a cold bias in northern Japan and a warm bias in southern Japan, indicating

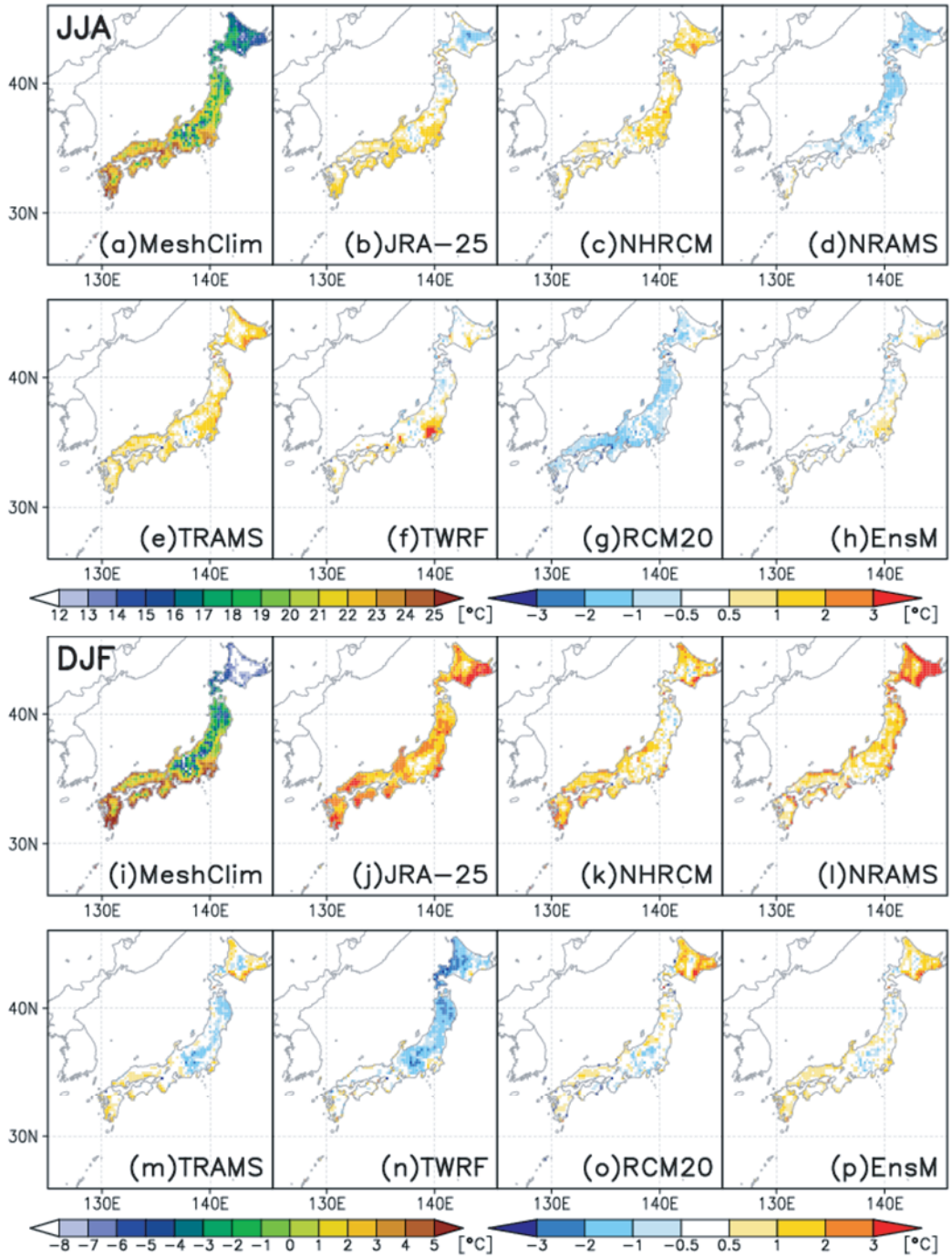

Fig. 2. (a) Climatological surface air temperatures averaged of for June, July, and August. The color shading is as the reference in the bottom of panels (e) and (f). (b–g) Surface temperature bias for (b) the JRA-25 reanalysis data, (c) NHRCM, (d) NRAMS, (e) TRAMS, (f) TWRF, and (g) RCM20. The color shading is as the reference in the bottom of panels (g) and (h). (h) Surface temperature bias for multi-model ensemble from (c) to (g). (i–p) Same as (a–h) but averaged for December, January, and February. Note that the meshed climatological data are calculated from 1971 to 2000, while the RCMs average is for from 1985 to 2004.

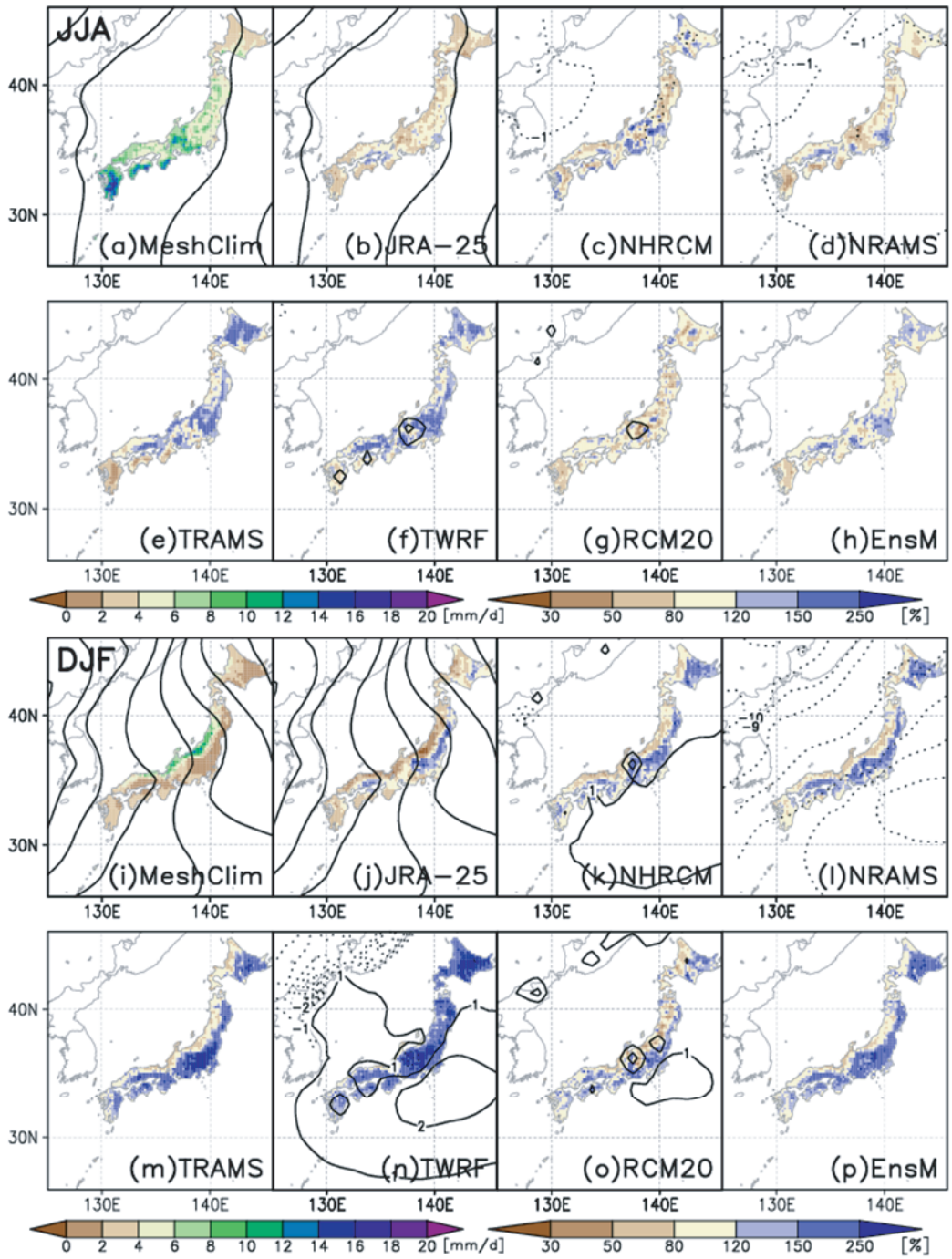

Fig. 3. Same as Fig. 2, but (shading) precipitation (mm day^{-1}) with (contour) sea level pressure (SLP; hPa). The contour interval is 2 hPa for (a, b, i, j) and 1 hPa for (c–h, k–p). Note that SLP for observation is derived from JRA-25 reanalysis. SLP of TRAMS is not available.

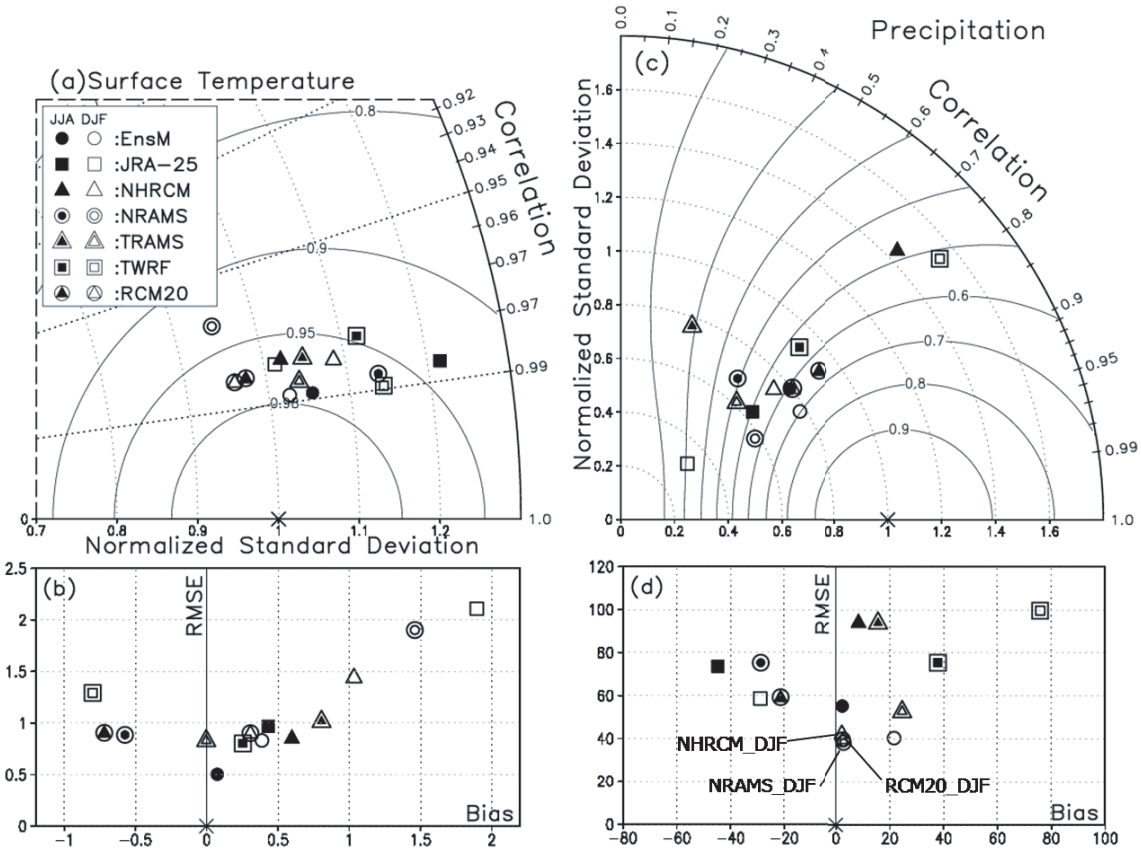

Fig. 4. (a) The Taylor diagram and (b) bias-RMSE scatter diagram for the surface temperatures. (c, d) Same as (a, b) but for precipitation. Symbol meaning can be found in the legend in the upper left corner in (a). Contour indicates Taylor's skill score.

that most of RCMs had a better skill than JRA-25. The simple ensemble mean of five RCMs much improved the skill, along with the model bias in summer and winter temperature.

The skill scores for summer precipitation are high (0.2–0.65; Fig. 4c) because of the moderate spatial correlation and weakly simulated contrast of the rainfall pattern, which is associated with the dry (wet) bias around the wet (dry) region in RCMs. The RMSE of RCMs exceeds 60 mm month^{-1} regardless of wet or dry bias (Fig. 4d). The skill scores for winter precipitation indicate that the spatial distribution of precipitation is largely improved by RCMs, while they still have small standard deviations compared to observations. The RCMs have comparable RMSE to that of JRA-25, although one RCM has a large bias of 100 mm month^{-1} due to overestimation bias. The ensemble mean of the RCMs has advantage over individual RCMs in the skill score, whereas it shows slight improvement in the RMSE for both seasons.

Figure 5 shows the scatter diagram of observation versus biases in climatological monthly temperature and precipitation averaged over 60 provinces throughout Japan (Appendix). When the observed temperature is higher than 0°C, the temperature biases range within 3 K for any month and any provinces. However, the warm bias is prominent below the freezing point. This is consistent with the warm bias in Hokkaido shown in Fig. 2 (see Subsection 4.1 for further discussion). The temperature bias above the freezing point is almost constant in NHRCM and TRAMS, whereas the other models show a cold bias instead. On the other hand, the precipitation plot shows that many RCMs overestimate weak rainfall and underestimate heavy rainfall, consistent with the behavior of the PRUDENCE models (Christensen et al. 2008). The TWRF model simulates winter precipitation

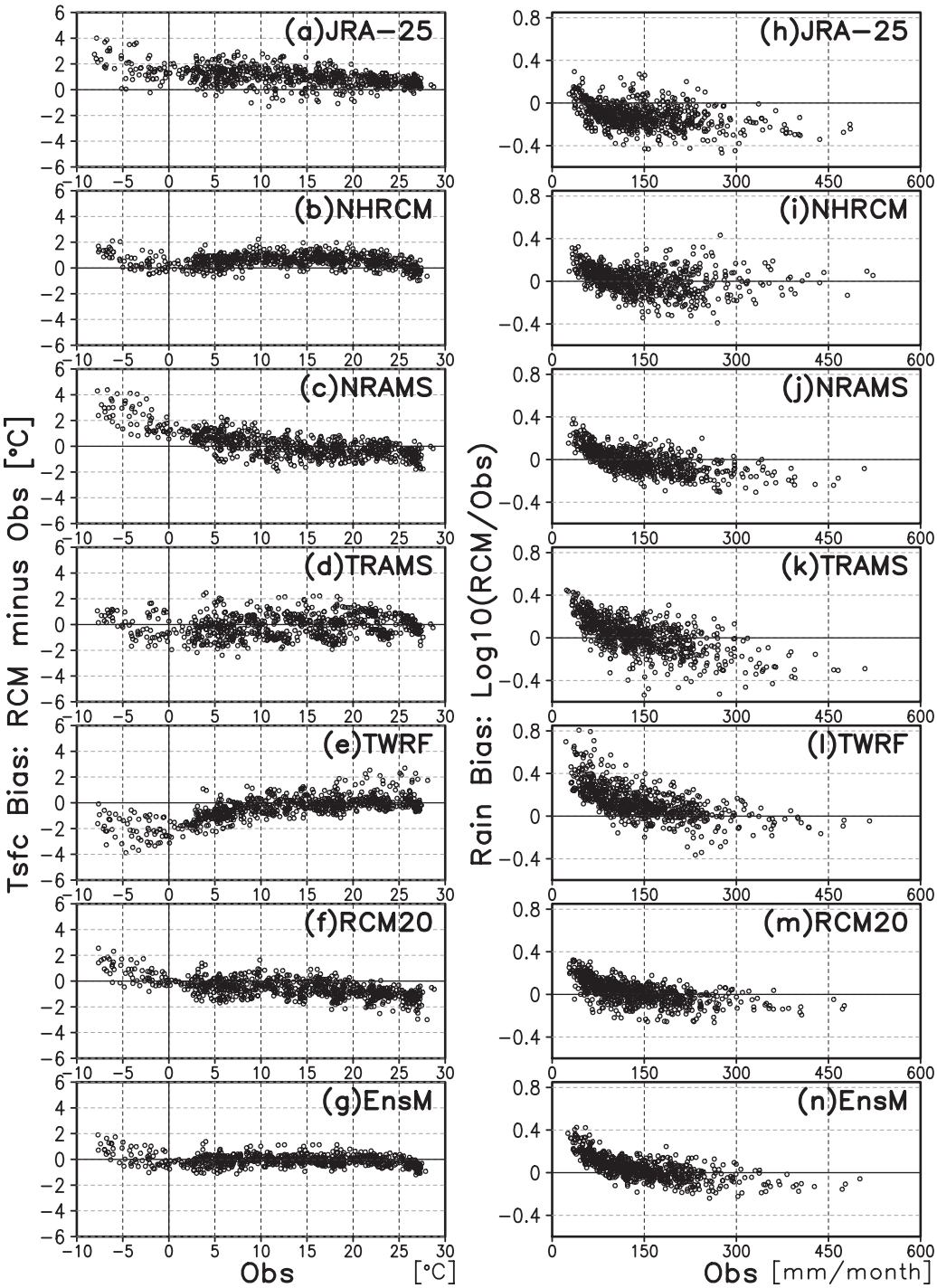

Fig. 5. The plot of the observation versus bias for monthly climatological (right) surface air temperatures and (right) precipitation for 60 Japanese provinces. The horizontal axis indicates the observation, and the vertical axis indicates the bias. The temperature bias is the difference from the observation and the precipitation bias is the common logarithm of precipitation amount ratio to the observation. (a, h) the JRA-25 reanalysis data, (b, i) NHRCM, (c, j) NRAMS, (d, k) TRAMS, (e, l) TWRF, (f, m) RCM20, and (g, n) multi-model ensemble of five RCMs.

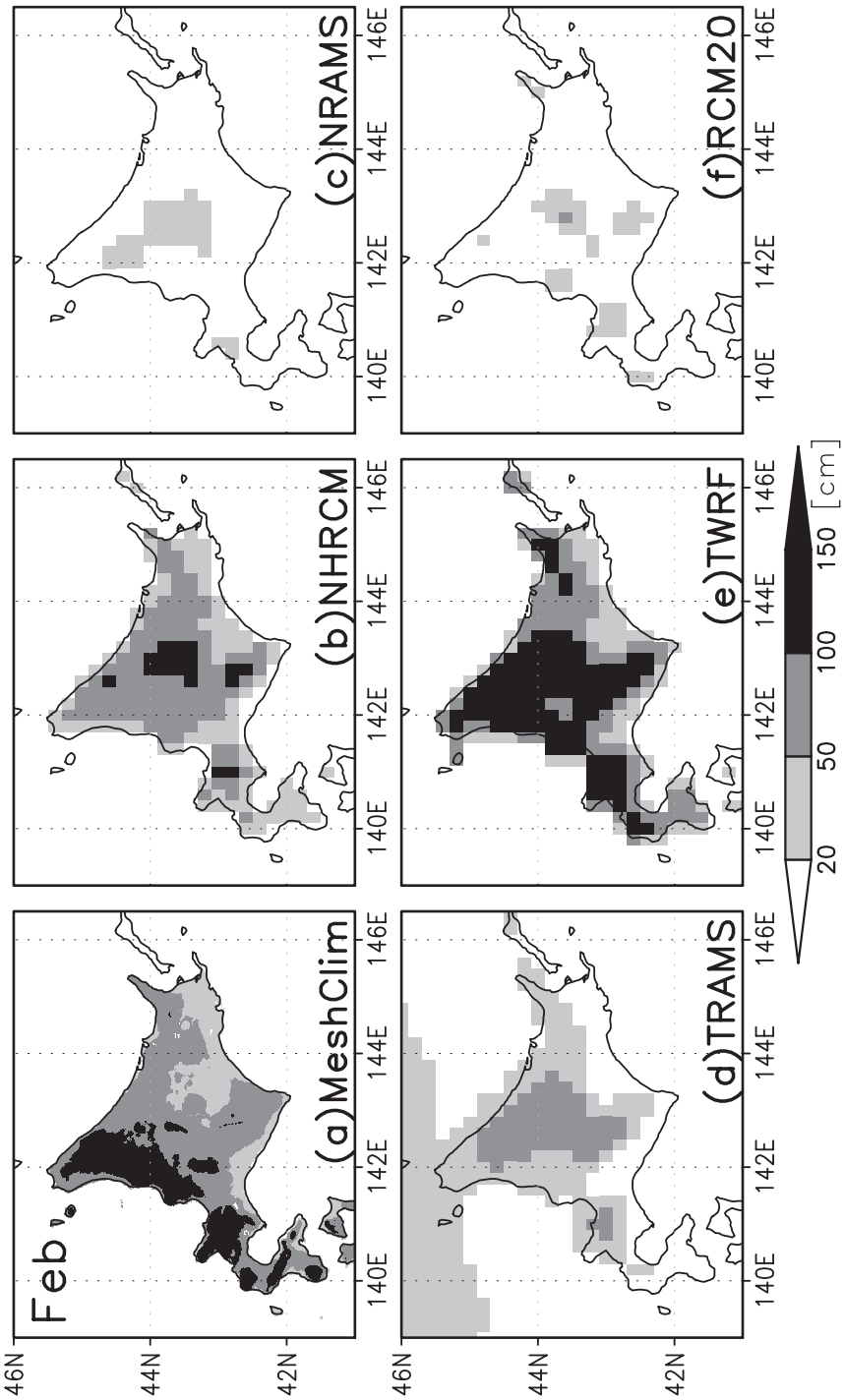

Fig. 6. The maximum snow depth (cm) in Hokkaido in February. (a) Observation, (b) NHRCM, (c) NRAMS, (d) TRAMS, (e) TWRF, and (f) RCM20. The shading is as the bottom reference. The snow water equivalent of TRAMS is converted to snow depth by assuming the density of 300 kg m^{-3} following Adachi et al. (2009).

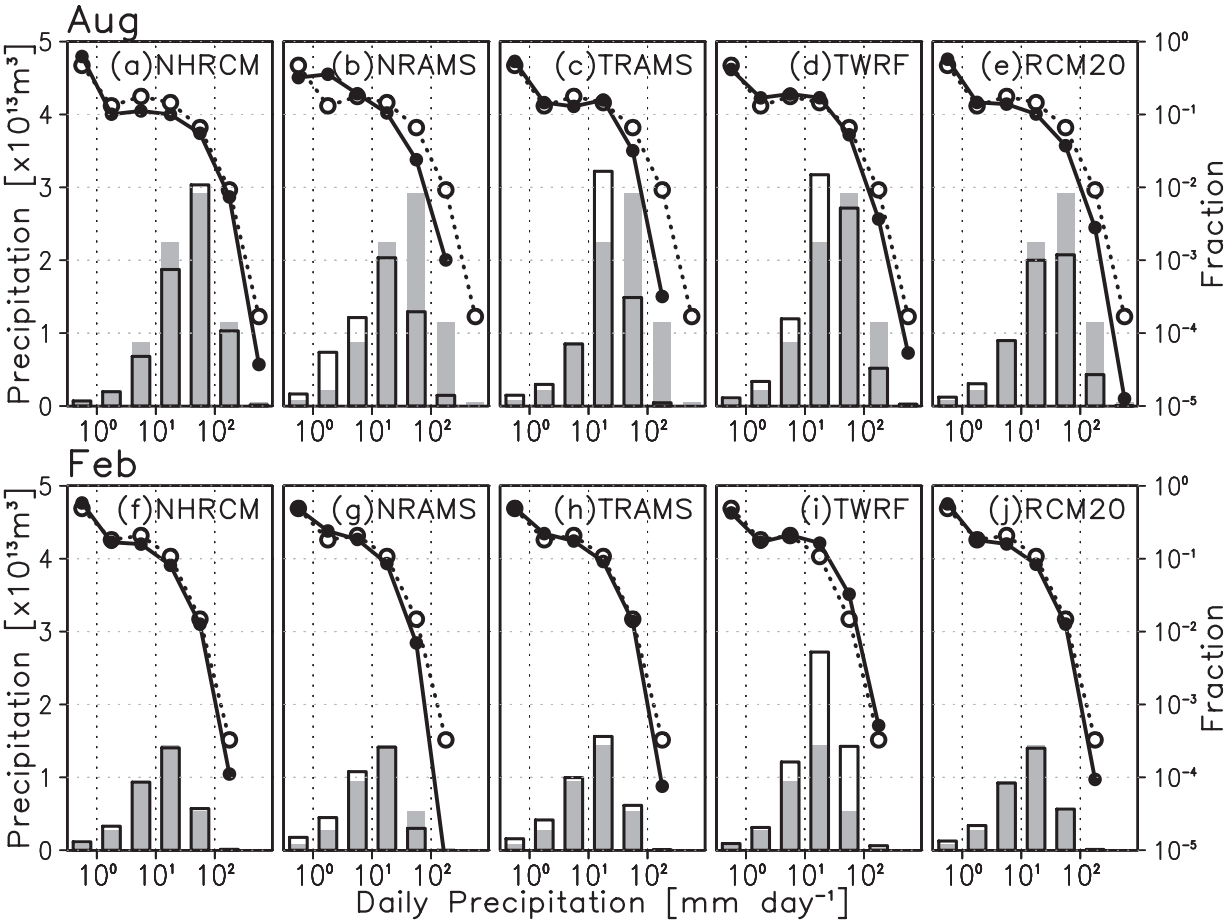

Fig. 7. Probability density function (lines with the right axis) and precipitation amount (bars with the left axis) binned to 0–1.0, 1.0–3.16, 3.16–10, 10–31.6, 31.6–100, 100–316, and more than 316 mm day^{-1} for August (a–e) and February (f–j). (a, f) NHRCM, (b, g) NRAMS, (c, h) TRAMS, (d, i) TWRF, and (e, j) RCM20. The references based on APHRO_JP are shown in the dashed line and in the gray bars for each panel.

almost 1.5 times larger than observation and has a relatively large bias, especially for dry months (< 80 mm month^{-1}). RCM20 and NRAMS show relatively small variability in model bias in monthly precipitation.

4. Discussion

4.1 Cause of RCM bias

Analyses of bias and skill in model outputs reveal that downscaling products using 20 km RCM add detailed information toward JRA-25. On the other hand, there seem to be some limitations in performance of RCMs when compared to observation. In this section, we examine the cause of biases and discuss a possibility of improvement.

The RCMs showed similar performances with small biases in the monthly surface temperature, whereas each RCM applies different land surfaceand turbulent closure models. Figure 5 showed a wide spread in warm biases in areas with a monthly-mean temperature lower than freezing, which is mainly observed in Hokkaido. This trend cannot be explained by a similar tendency in the parent model because the information from JRA-25 comes through the boundary of the domain. Because the bias is commonly seen in most RCMs, it is unlikely that the land surface model is responsible for the temperature bias. Comparison of SST distribution around Hokkaido among several datasets indicates that SST pattern in JRA-25 is also not responsible for the warm bias (figure not shown). Generally, a warm bias and an underestimation of snow accumulation coincide

due to the ice-albedo feedback that indicates net shortwave radiation will decrease over the snow surface because of high albedo. Because energy is expended to melt and warm the snow layer, sensible heat flux from the surface will also decrease. Rasmussen et al. (2011) and Ikeda et al. (2010) revealed that simulated snow accumulation depends on the spatial resolution of RCM, and a high resolution RCM with a horizontal mesh size of several kilometers can reasonably simulate the snow amount.

In our experiments, the RCMs present snow cover in Hokkaido during the winter season, but their spatial pattern and depth are quite different from those of the observed (Fig. 6). All RCMs, except TWRF, obviously underestimate the amount of snow depth. The snow is distributed mainly over high mountains located in central Hokkaido instead of the western part (see Fig. 1). Sensible heat flux is indeed negative over snow areas in RCMs, while it turns out to be positive in the snow free regions where the land surface warms the atmosphere. Thus, one of the possible reasons for the warm bias is the underestimation in snow values in 20-km mesh RCMs. In other words, the warm bias over snow areas is regarded as a typical problem of 20-km mesh model. The snow simulation and resultant warm bias will be improved in experiments with a higher resolution model in which more realistic vertical motion and realistic representation of process in the boundary layer are solved. The peculiar temperature bias of TWRF probably reflects overestimation of the precipitation.

On the other hand, the precipitation bias seems to be related to cumulus parameterization schemes. In our experiments, three of the RCMs use Kain-Fritsch (K-F) scheme, while the other two models apply Arakawa-Schubert (A-S) scheme. The K-F scheme in NHRCM is implanted from WRF-ARW. In the trigger function of the K-F scheme, a temperature increment concept is added to simulate local perturbation forcing as a function of grid-scale updraft. A large temperature increment will generally lead to large sub-grid scale perturbation and resultant shallow convection. To prevent excessive temperature increment associated with grid-scale motion, factor offset is modified in NHRCM (Saito et al. 2006). In addition to the perturbation due to grid-scale motion, perturbation dependent upon relative humidity is also introduced in the trigger function in NHRCM (Saito et al. 2007) to improve the overestimation of convective rain induced by orography.

From this point of view, there is a considerable difference in precipitation features among these two models. Figure 7 shows the probability density function and precipitation amounts in seven categories of precipitation in August and February. NHRCM reproduces intense precipitation relatively well (Fig. 7a), while the contribution of precipitation less than 31.2 mm day^{-1} is too large in TWRF (Fig. 7d). For the winter season, NHRCM captures the precipitation amount in each category of intensity well, while TWRF overestimates precipitation amounts in all categories. The results indicate that adjustment within the cumulus parameterization scheme leads to a large difference in precipitation intensity as much as due to difference of parameterization scheme.

Nevertheless, the RCMs tend to have an underestimation bias for heavy rain and overestimation bias for the weak rain. Two RAMSs and RCM20 underestimate the amount of intense precipitation during summer (Figs. 7b, c, e). For the winter season, NHRCM and RCM20 provide frequent instances of weak rainfall of less than 1 mm day^{-1}, while NRAMS and TRAMS overestimate precipitation with an intensity of 1 mm to 3.2 mm day^{-1} (Figs. 7f–j). It is known that RCM tends to overestimate weak rainfall, known as "drizzle problem" (e.g., Gutowski et al. 2003; Fowler and Kilsby 2007). Since the precipitation is often associated with the orographic effect, orography representation also seems to affect precipitation features. For extensive application of downscaling products, it is important to adequately simulate not only total precipitation but also its intensity. Continuous effort using several sensitivity experiments is required to improve the model.

4.2 Advantage of using RCM

The RCM is expected to have better performance than that of coarse-grid GCM with regards to reproducing the phenomena that are associated with the geographical structure and that have meso-scale mechanisms. Improved skill scores in surface temperature and precipitation in the RCMs, compared to that of JRA-25, is generally due to better representation of the spatial variability, which suggests that the both dynamical and physical effects of RCM may contribute to the performance of mean state especially for precipitation.

In order to confirm the effect of fine geographical distribution in RCM on extreme events, Yamase is compared as a typical example, which is characterized by cold and moist winds associated with the appearance of the Okhotsk High—a blocking anticyclone—during summer. Figure 8 shows the performance of RCMs in a Yamase event in the summer of 1993 which is the coldest summer in 1985–2004 due to a robustly developed Okhotsk high (e.g., Kanno 1995; Kodama 1997). The RCMs are able to simulate the general features of the situation (Figs. 8c–g); the intensity of the cold anti-

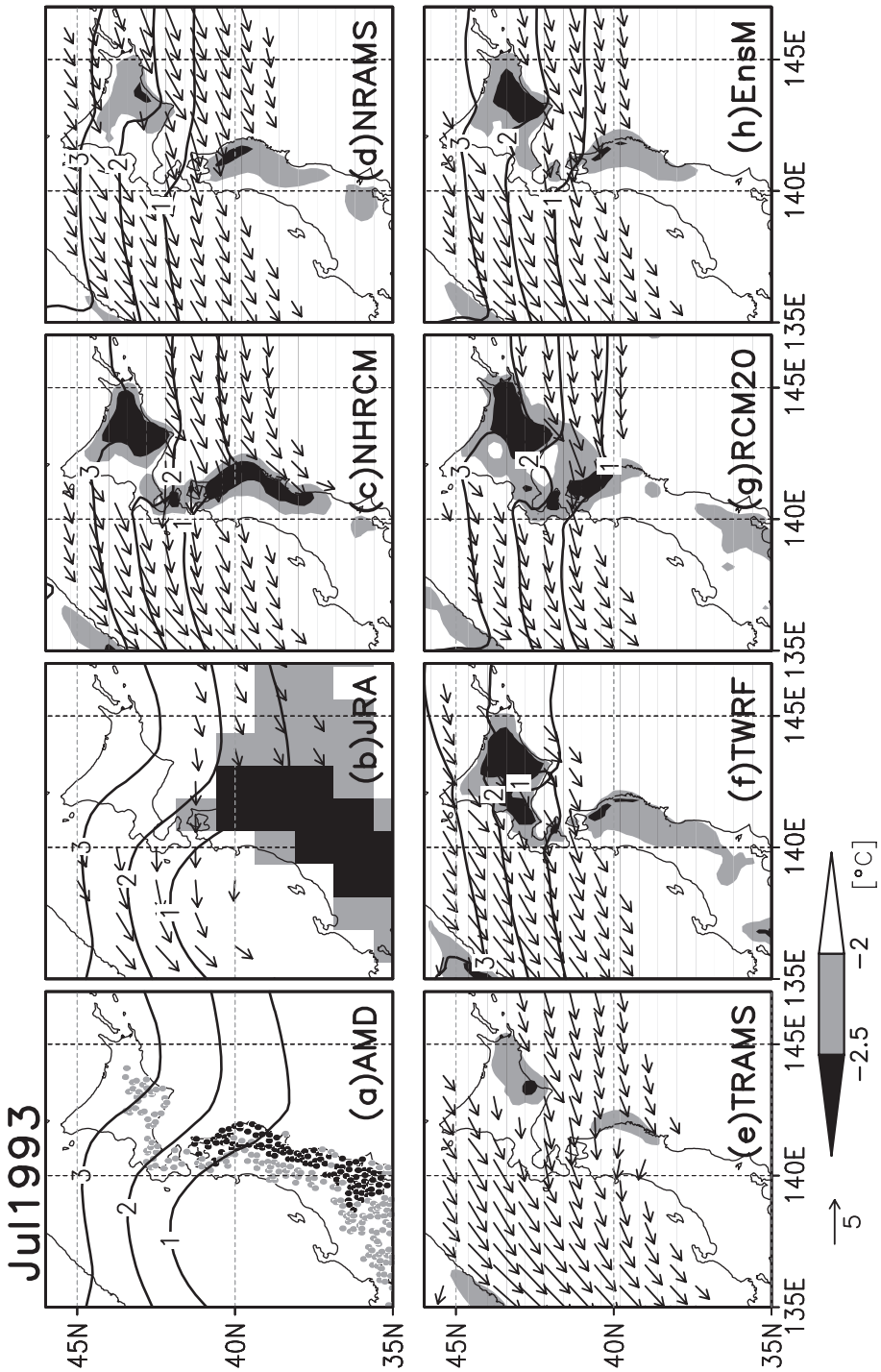

Fig. 8. The anomaly from the 20-year mean of surface air temperatures and SLPs in July, superimposed with the wind anomalies larger than 2 m s^{-1} for (b)–(h). (a) Observed anomaly of AMeDAS and SLP derived from JRA-25. The SLP for TRAMS is not available.

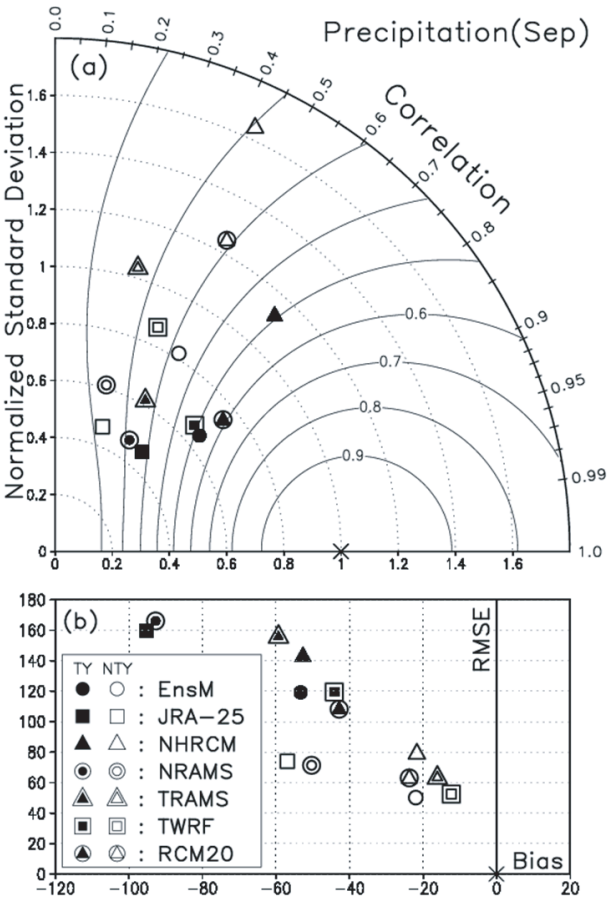

Fig. 9. Same as Fig. 4, but for typhoon period (TY) and non-typhoon period (NTY) in September. See text for the definition of TY and NTY. The meaning of marks is as the legend in the lower left corner in (b).

cyclonic system and the temperature of the RCMs are similar to those observed. The modeled temperature on the Pacific side of Japan is more than 2.0°C colder than that of the Japan Sea side at around 40°N, and unclear temperature contrast at the mountains in JRA-25 is improved. The Yamase case suggests that the reproducibility of other meso-scale phenomena related to the mechanical effect of the topography (e.g., foehn, snow accumulation) would be also be improved by using RCMs. The misplaced pressure anomaly leads to weak cold anomalies, which are attributed to the fact that the RCM domain covers only part of the Okhotsk High. It should be noted that both the representation of geographical features in RCM and the triggering large-scale circulation are crucial to correctly reproduce local weather conditions.

Meanwhile the advantage in RCMs being able to resolve meso-scale processes for extreme events is investigated using typhoons (e.g., Feser and von Storch 2008), which often brings heavy rainsin excess of 100 mm day^{-1}. Although approaching typhoons are few in number and move along different paths in each case, each has a great impact on the local climatology due to strong winds and heavy rainfall. This also makes it difficult to investigate the statistics. As demonstrated by many studies, the model with coarse mesh size cannot represent a detailed typhoon structure, which is generally improved by advancements in spatial resolution (Bengtsson et al. 2007; Murakami and Sugi 2010). Location and typhoon tracks in this work are well simulated even without nudging systems, while minimum typhoon pressure is overestimated (figure not shown). In addition to the inadequacy in spatial resolution, analysis on the development of typhoons in RCMs indicated that the weak intensity of a simulated typhoon is attributed to a domain size that is too narrow for them to fully deepen.

According to the JMA, the monthly number of typhoons approaching the Japan islands between 1985 and 2004 was highest in September. We divide the days of September into two categories and compare the skill score and RMSE of precipitation in each season; typhoon (TY) cases are when a typhoon exists within 300 km from a Japanese land area, the other is non-typhoon (NTY) case. TY accounts for 35.7% according to JMA best track data. All RCMs underestimate precipitation in both cases (Fig. 9), and larger negative biases are found in TY period due to underestimation bias for intense precipitation. Interestingly, RCMs exhibit much better skill during TY due to spatial correlation, which reveals 0.35 to 0.5 in NTY and 0.5 to 0.8 in TY, while RMSE in TY is 1.5 to 2 times of that in NTY. In situations which typhoons or disturbances move across Japan, 20 km RCMs can suitably simulate the precipitation zone, and show relatively better skill scores because the climate field is dominated largely by the large-scale system. During NTY cases, on the other hand, skill becomes worse due to the overestimation in weak rainfall and disagreement in location. Relatively small spatial variability and larger RMSEs in TY case suggest that we somewhat benefit from high resolution RCMs that incorporate small-scale processes with the detailed orographic effect with 20 km grid spacing 20 km, though RCMs may have limited effect on the performance of RCMs in the typhoon simulation.

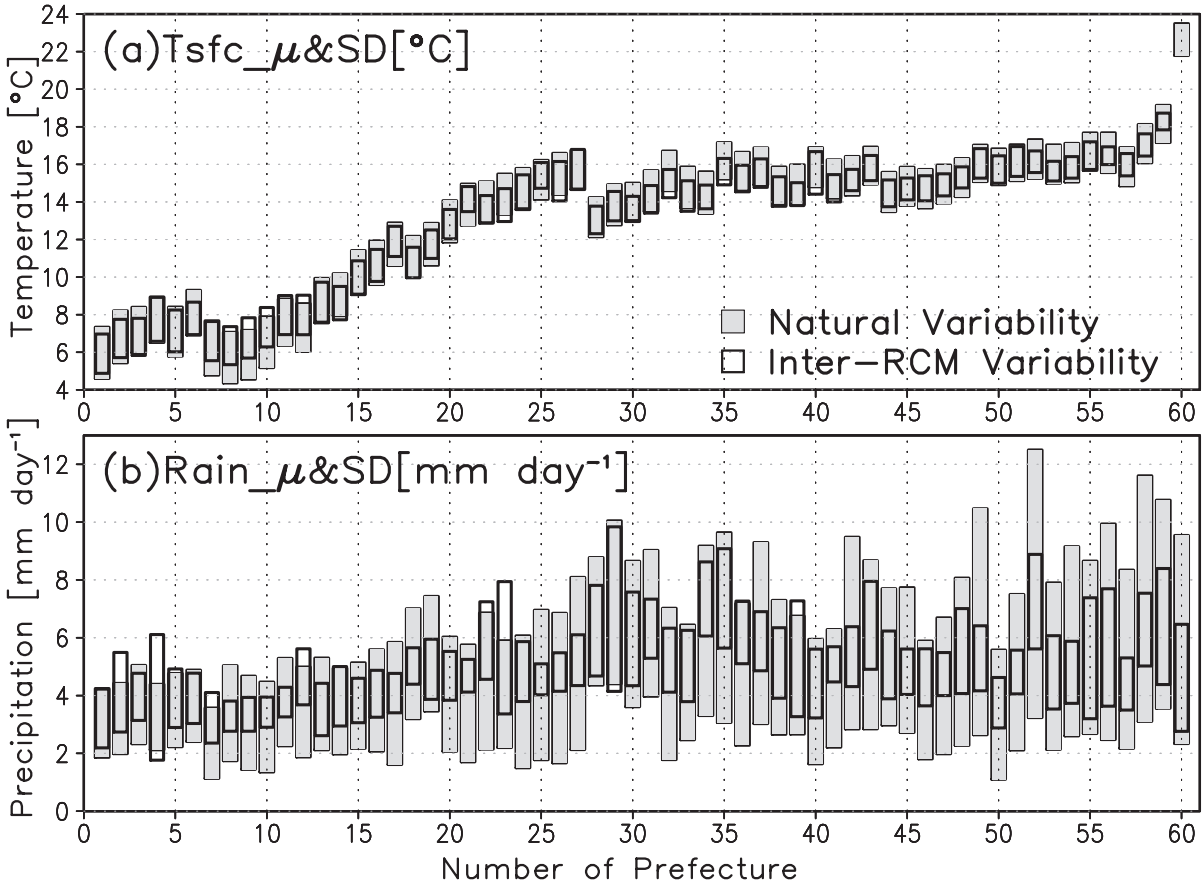

Fig. 10. The standard deviation in monthly regional (a) temperature and (b) precipitation for the natural variability (gray-solid bars) and inter-RCM variability (open bars). Each bar ranges within one standard deviation from the average. The horizontal axis means the number of province (Appendix).

4.3 Multi-RCM ensemble

This study demonstrated that multi-model ensemble mean has a small bias in surface air temperature and precipitation over Japan (Figs. 2, 3). The skill score and error within the ensemble mean for Japan generally reveal an improved performance (Fig. 4). This is associated with the magnitude of bias that is comparable among RCMs for many locations and the distributed model values centering around the observed value. The ensemble approach is also validated for narrower Japanese provinces. Figure 10 shows the range of natural variability, defined by the variance of monthly values for 20 years and the range of inter-RCM variability for 60 provinces. The median gray bars in Fig. 10 shows the observed climatology, and the open bars indicate the multi-model ensemble average. The multi-model ensemble mean reveals good agreement with the observation in each province as demonstrated by Figs. 5g and n. The results of the multi-model ensemble are consistent with many other studies in other regions (Jacob et al. 2007; de Castro et al. 2007; Gutowski et al. 2010). The results reinforce the usefulness and necessity of multi-RCM ensembles. The ensemble mean even shows similar biases for strong precipitation and cold temperature as do many other models, as described above. For example, the ensemble mean tends to overestimate rainfall over eastern and central Japan, and to underestimate rainfall over Kyushu Island (prefectures Nos. 53–59).

A small spread in the RCM results should be expected if large-scale forcing strongly controls the regional climate variability, regardless of the performance of the parent model. However, since regional climate is not controlled solely by large-scale forcing from lateral boundary condition, each RCM shows spatiotem-

porally differences in bias distribution. The spread of RCM results originates from differences in dynamical basis, physical schemes, and parameterizations. These schemes are essentially set for the purpose of reproducing realistic regional detail. The ensemble mean of such RCMs is naturally expected to show good performance (Hagemann and Jacob 2007). Even though the RCMs performances are not sufficient, choosing five RCMs to construct an ensemble mean results in successful performance thanks to fortunate coincidence.

If the standard deviation in inter-RCM variation becomes quite large, it undermines confidence in individual RCM results, even though the ensemble mean agrees with observation. The influence of the synoptic scale forcing also contributes to the spread of RCM results, and thus the inter-RCM variability depends on countries or season (Rockel et al. 2008; Rinke and Dethloff 2000). Here we compare the inter-RCM variability with standard natural deviation for each region to observe the spread in RCM simulations (Fig. 10). There is considerable spread among the RCM simulations, both of temperature and precipitation, which suggests RCM uncertainty. The standard deviations within the inter-RCM variability are essentially smaller than those of natural variability. Because the observed natural variability of the monthly regional value can be captured by the RCMs (figure not shown), the individual RCM results will simply be corrected using a bias correction tool (e.g., Christensen et al. 2008). The 60 sub-regional mean values derived from 20 km RCMs can be provided to the impact assessment group for various application studies.

The ensemble mean process may make the local signal obscured in cases which reproducibility of the event partly depends on representation of orographic structures, like Yamase (Fig. 8), because the orographic structures of RCMs are different each other. We should mention that variations in shorter time scales or finer spatial scales may show a large diversity among RCMs, so the averaging of RCMs obscures small-scale signals. The features that are common to the RCMs (e.g., a warm bias at temperatures below freezing) should also be interpreted with caution. The mechanism studies should be conducted with individual RCM simulations, while the ensemble mean value is favorable for several impact studies as long as the characteristics of the RCMs are understood. Inter-comparison processes provide us with the additional information as to the uncertainty or confidence level of RCM results. This procedure would be important in ensuring the reliability of output prior to discussing projection results.

5. Conclusion

In this study, the downscaling products for a Japanese climate using five 20-km meshed RCMs with boundary conditions given from the JRA-25 reanalysis are analyzed. All RCMs successfully reproduce general spatiotemporal distribution features in temperature and precipitation. The regional averaged biases for 60 Japanese provinces range within 3°C for the monthly temperature, and from 0.5 to 2 times for monthly rainfall.

The spatial distributions of bias in the surface temperature are independent of the geographical distribution, and the RCMs can reduce the errors. The spatial correlation in temperature is very high (more than 0.95), which leads to high skill scores. The ensemble mean further improves skill score and reduces bias, while the warm bias remains in areas with a monthly-mean temperature lower than freezing. This bias is probably due to the lack of spatial resolution in the RCM and, consequently, the snow underestimation.

JRA-25 underestimates the precipitation amounts for the summer and winter season, but the 20-km meshed RCMs improve the bias. The models underestimate heavy rains for the Pacific Ocean side of southern Japan during summer and Japan Sea side in winter. One possible reason for that is the adjustment of convective parameterization scheme. The dry bias of heavy rains may affect the overall balance in precipitation for each intensity category.

The advantage of dynamical downscaling using RCMs over the parent model can be confirmed through their orographic effects (e.g., Yamase). Although small-scale processes can be simulated in the 20-km mesh RCMs, they have limited effect on the performance of RCMs as indicated by skill score during typhoon period. Furthermore, the ensemble process enables us to recognize the robustness of detailed information added by RCMs. The ensemble mean using five RCMs reveals great performance by compensating for the inherent biases of individual RCMs. There is considerable spread in the RCM results, while the standard deviation in inter-RCM variability for the monthly mean values for 60 Japanese provinces are smaller than those of inter-annual variability. It indicates that the multi-RCM ensemble mean for each province, surface temperature and precipitation values, will be simply corrected by some bias correction method and could be utilized in impact assessment studies as long as the characteristics of the RCMs are understood. Note that the multi-RCM ensemble mean does not always produce the best estimate if the performance depends on spatial resolution, domain size, and representation of topography. This pa-

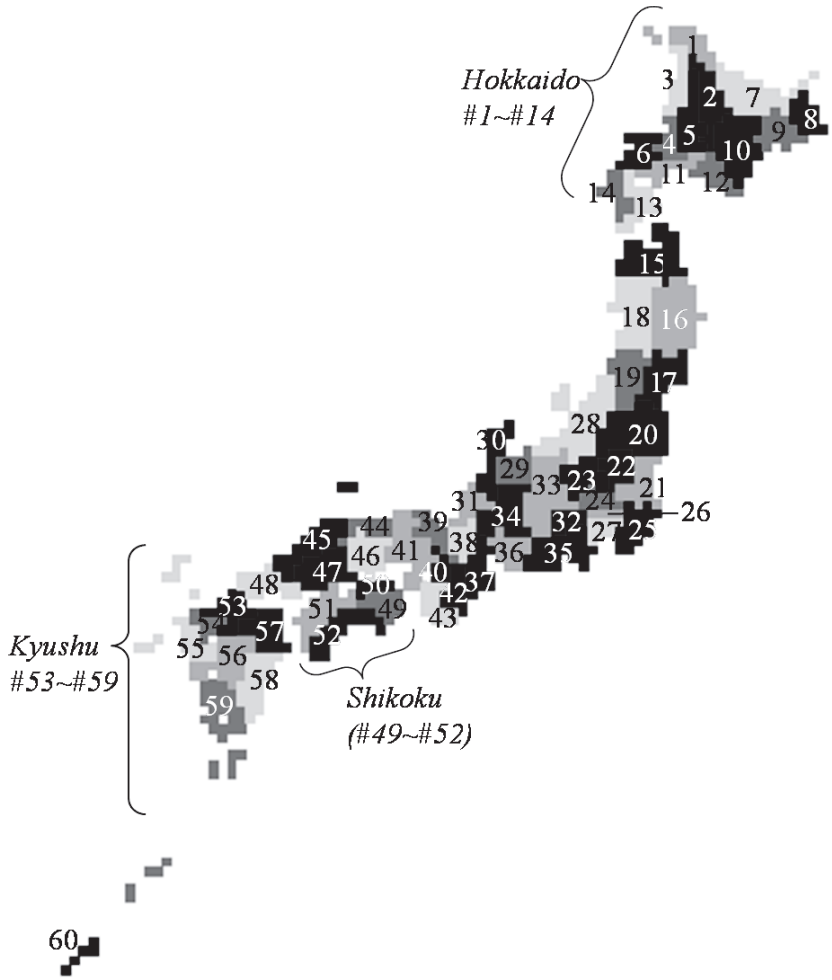

Fig. A. The number and name of 60 Japanese provinces.

per will help to ensure accurate understanding of downscaling results for future projections.

Acknowledgements

The authors express their sincere gratitude to two anonymous referees and editor for their valuable comments and suggestions. This study was supported by the Global Environment Research Fund (S-5-3) of the Ministry of the Environment, Japan. This work is part of a PhD thesis by the first author, submitted to the University of Tsukuba, for which thanks are due to Prof. H. L. Tanaka, Prof. F. Kimura, Prof. H. Kusaka, and Prof. F. Fujibe.

Appendix

The Appendix stands to explain the geographical location and the name of the 60 Japanese provinces (Fig. A). Each occupies 1,900 to 15,300 km^2. Hokkaido contains Nos. 1–14, Shikoku Nos. 49–52, and Kyusyu Nos. 53–59.

References

Adachi, A. S., F. Kimura, and M. Tanaka, 2009: Reproducibility of past 20 years climate using dynamical downscaling method and future prediction of snow cover in winter. *Terrestrial Environment Research Center Report*, **10**, 51–60.

Arakawa, A., and W. H. Schubert, 1974: Interaction of a cumulus cloud ensemble with the large-scale environ-

ment. Part I. *J. Atmos. Sci.*, **31**, 674–701.

Bengtsson, L., K. Hodges, M. Esch, N. Keenlyside, L. Kornblueh, J.-J. Luo, and T. Yamagata, 2007: How may tropical cyclones change in a warmer climate? *Tellus*, **59A**, 539–561.

Castro, C. L., R. A. Pielke Sr., and G. Leoncini, 2005: Dynamical downscaling: Assessment of value retained and added using the Regional Atmospheric Modeling System (RAMS). *J. Geophys. Res.*, **110**, 10.1029/2004JD004721.

de Castro, M., C. Gallardo, K. Jylha, and H. Tuomenvirta, 2007: The use of a climate-type classification for assessing climate change effects in Europe from an ensemble of nine regional climate models. *Clim. Change*, **81**, 329–341.

Christensen, J. H., F. Boberg, O. B. Christensen, and P. L. Picher, 2008: On the need for bias correction of regional climate change projections of temperature and precipitation. *Geophys. Res. Lett.*, **35**, doi:10.1029/2008GL035694.

Christensen, J. H., M. Rummukainen, and G. Lenderink, 2009: Formulation of very-high-resolution regional climate model ensembles for Europe. *ENSEMBLES: Climate Change and Its Impacts: Summary of Research and Results from the ENSEMBLES Project* Van der Linden, P., and J. F. B. Mitchell, Eds., Met Office Hadley Centre, Exeter, UK, 47–58.

Christensen, O. B., M. A. Gaertner, J. A. Prego, and J. Polcher, 2001: Internal variability of regional climate models. *Clim. Dyn.*, **17**, 875–887.

Deque, M., D. P. Rowell, D. Luthi, F. Giorgi, J. H. Christensen, B. Rockel, D. Jacob, E. Kjellstrom, M. de Castro, and B. van den Hurk, 2007: An intercomparison of regional climate simulations for Europe: assessing uncertainties in model projections. *Clim. Change*, **81**, 53–70.

Dickinson, R. E., A. Henderson-Sellers, and P. Kennedy, 1993: Biosphere atmosphere transfer scheme (BATS) version le as coupled to the NCAR Community Climate Model, *NCAR Tech. Note, NCAR/TN-387+STR*, Natl. Cent. for Atmos. Res., Boulder, Colo.

Eastman, J. L., M. B. Coughenor, and R. A. Pielke Sr., 2001: The regional effects of CO_2 and landscape change using a coupled plant and meteorological model. *Global Change Biol.*, **7**, 797–815.

Ek, M. B., K. E. Mitchell, Y. Lin, E. Rogers, P. Grunmann, V. Koren, G. Gayno, and J. D. Tarpley, 2003: Implementation of Noah land surface model advances in the National Centers for Environmental Prediction operational mesoscale Eta model. *J. Geophys. Res.*, **108**, doi:10.1029/2002JD003296.

Feser, F., and H. von Storch, 2008: A dynamical downscaling case study for typhoons in southeast Asia using a regional climate model. *Mon. Wea. Rev.*, **136**, 1806–1815.

Fowler, H. J., and C. G. Kilsby, 2007: Using regional climate model data to simulate historical and future river flows in northwest England. *Clim. Change*, **80**, 337–367.

Fu, C., S. Wang, Z. Xiong, W. Gutowski, D.-K. Lee, J. L. McGregor, Y. Sato, H. Kato, J.-W. Kim, and M.-S. Suh, 2005: Regional climate model intercomparison project for Asia. *Bull. Amer. Meteor. Soc.*, **77**, 437–471.

Giorgi, F., and G. T. Bates, 1989: The climatological skill of a regional model over complex terrain. *Mon. Wea. Rev.*, **117**, 2325–2347.

Giorgi, F., 1990: Simulation of regional climate using a limited area model nested in general circulation model. *J. Climate*, **3**, 941–963.

Giorgi, F., and R. Francisco, 2000: Evaluating uncertainties in the prediction of regional climate change. *Geophys. Res. Lett.*, **27**, 1295–1298.

Giorgi, F., C. Jones, and G. R. Asrar, 2009: Addressing climate information needs at the regional level: the CORDEC framework. *WMO Bulletin*, **58**, 175–183.

Gutowski, W. J., S. G. Decker, R. A. Donavon, Z. Pan, R. W. Arritt, and E. S. Takle, 2003: Temporal-Spatial Scales of Observed and Simulated Precipitation in Central U.S. Climate. *J. Climate*, **16**, 3841–3847.

Gutowski, W. J., R. W. Arritt, S. Kawazoe, D. M. Flory, E. S. Takle, S. Biner, D. Caya, R. G. Jones, R. Laprise, L. R. Leung, L. O. Mearns, W. Moufouma-Okia, A. M. B. Nunes, Y. Qian, J. O. Roads, L. C. Sloan, and M. A. Snyder, 2010: Regional Extreme Monthly Precipitation Simulated by NARCCAP RCMs. *J. Hydrometeor.*, **11**, 1373–1379.

Hagemann, S., and D. Jacob, 2007: Gradient in the climate change signal of European discharge predicted by a multi-model ensemble. *Clim. Change*, **81**, 309–327.

Hirai, M., T. Sakashita, H. Kitagawa, T. Tsuyuki, M. Hosaka, and M. Oh'izumi, 2007: Development and validation of a new land surface model for JMA's operational global model using the CEOP observation dataset. *J. Meteor. Soc. Japan*, **85A**, 1–24.

Ikeda, K., R. Rasmussen, C. Liu, D. Gochis, D. Yates, F. Chen, M. Tewari, M. Barlage, J. Dudhia, K. Miller, K. Arsenault, V. Grubišić, G. Thompson, and E. Guttman, 2010: Simulation of seasonal snowfall over Colorado. *Atmos. Res.*, **97**, 462–477.

Ishizaki, N., and I. Takayabu, 2009: On the warming events over Toyama Plain by using NHRCM. *SOLA*, **5**, 129–132.

Jacob, D., L. Bärring, O. B. Christensen, J. H. Christensen, M. Castro, M. Déqué, F. Giorgi, S. Hagemann, M. Hirschi, R. Jones, E. Kjellström, G. Lenderink, B. Rockel, E. Sánchez, C. Schär, S. I. Seneviratne, S. Somot, A. Ulden, and B. Hurk, 2007: An inter-comparison of regional climate models for Europe: model performance in present-day climate. *Clim. Change*, **81**, 31–52.

Kain, J., and J. Fritsch, 1993: Convective parameterization for mesoscale models: The Kain-Fritsch scheme. *The Representation of Cumulus Convection in Numerical Models, Meteor. Monogr.*, **46**, Amer. Meteor. Soc., 165–170.

Kamiguchi, K., O. Arakawa, A. Kitoh, A. Yatagai, A.

Hamada, and N.Yasutomi, 2010: Development of APHRO_JP, the first Japanese high-resolution daily precipitation product for more than 100 years. *Hydrological Research Letters*, **4**, 60–64.

Kanamitsu, M., and H. Kanamaru, 2007: Fifty-seven-year California reanalysis downscaling at 10 km (CaRD10). Part I: System detail and validation with observations. *J. Climate*, **20**, 5553–5571.

Kanno, H., 1995: On vertical structure of the Yamase in 1993, Extended abstract of the Yamase Symposium—'93 Yamase and its surroundings—, 163–167 (in Japanese).

Kida, H., T. Koide, H. Sasaki, and M. Chiba, 1991: A new approach for coupling a limited area model to a GCM for regional climate simulations. *J. Meteor. Soc. Japan*, **69**, 723–328.

Kodama, Y. M., 1997: Airmass transformation of the Yamase air-flow in the summer of 1993. *J. Meteor. Soc. Japan*, **75**, 737–751.

Kunkel, K. E., K. Andsager, X.-Z. Liang, R. W. Arritt, E. S. Takle, W. J. Gutowski Jr., and Z. Pan, 2002: Observations and regional climate model simulations of heavy precipitation events and seasonal anomalies: a comparison. *J. Hydrometeor.*, **3**, 322–334.

Kurihara, K., K. Ishihara, H. Sasaki, Y. Fukuyama, H. Saitou, I. Takayabu, K. Murazaki, Y. Sato, S. Yukimoto, and A. Noda, 2005: Projection of climatic change over Japan due to global warming by High-Resolution Regional Climate Model in MRI. *SOLA*, **1**, 97–100.

Leung, L. R., and S. J. Ghan, 1995: A subgrid parameterization of orographic precipitation. *Theor. Appl. Climatol.*, **52**, 95–118.

Mearns, L. O., F. Giorgi, L. McDaniel, and C. Shields, 1995: Analysis of daily precipitation variability in a nested regional climate model: Comparison with observations and 2XCO2 results. *Global and Planetary Change*, **10**, 55–78.

Murakami, H., and M. Sugi, 2010: Effect of model resolution on tropical cyclone climate projections. *SOLA*, **6**, 73–76.

Murazaki, K., H. Sasaki, H. Tsujino, I Takayabu, Y. Sato, H. Ishizaki, and K. Kurihara, 2005: Projection of climatic change over Japan due to global warming by High-Resolution Regional Climate Model in MRI. *SOLA*, **1**, 101–104.

Onogi, K., J. Tsutsui, H. Koide, M. Sakamoto, S. Kobayashi, H. Hatsushika, T. Matsumoto, N. Yamazaki, H. Kamahori, K. Takahashi, S. Kadokura, K. Wada, K. Kato, R. Oyama, T. Ose, N. Mannoji, and R. Taira, 2007: The JRA-25 reanalysis. *J. Meteor. Soc. Japan*, **85**, 369–432.

Pielke, R. A., W. R. Cotton, R. L. Walko, C. J. Tremback, W. A. Lyons, L. D. Grasso, M. E. Nicholls, M. D. Moran, D. A. Wesley, T. J. Lee, and J. H. Copeland, 1992: A comprehensive meteorological modeling system-RAMS. *Meteor. Atmos. Phys.*, **49**, 69–91.

Rasmussen, R., C. Liu, K. Ikeda, D. Gochis, D. Yates, F. Chen, M. Tewari, M. Barlage, J. Dudhia, W. Yu, K. Miller, K. Arsenault, V, Grubišić, G. Thompson, and E. Gutmann, 2011: High-resolution coupled climate runoff simulation of seasonal snowfall over Colorado: A process study of current and warmer climate. *J. Climate*, **24**, 3015–3048.

Rinke, A., and K. Dethloff, 2000: On the sensitivity of a regional Arctic climate model to initial and boundary conditions. *Climate Res.*, **14**, 101–113.

Rockel, B., C. L. Castro, R. A. Pielke Sr., H. von Storch, and G. Lencini, 2008: Dynamical downscaling: Assessment of model system dependent retained and added variability for two different regional climate models. *J. Geophys. Res.*, **113**, D21107, doi:10.1029/2007JD009461.

Rowell, D. P., 2006: A demonstration of the uncertainty in projections of UK climate change resulting from regional model formulation. *Clim. Change*, **79**, 243–257.

Rummukainen, M., 2009: State-of-the-art with regional climate models. *Wiley Interdisciplinary Reviews: Clim. Change*, **1**, 82–96.

Saito, K., F. Tsukasa, Y. Yamada, J. Ishida, Y. Kumagai, K. Aranami, S. Ohmori, R. Nagasawa, S. Kumagai, C. Muroi, T. Kato, H. Eito, and Y. Yamazaki, 2006: The operational JMA nonhydrostatic mesoscale model. *Mon. Wea. Rev.*, **134**, 1266–1298.

Saito, K., J. Ishida, K. Aranami, T. Hara, T. Segawa, M. Narita, and Y. Honda, 2007: Nonhydrostatic atmospheric models and operational development at JMA. *J. Meteor. Soc. Japan*, **85B**, 271–304.

Sakamoto, T. T., Y. Komuro, T. Nishimura, M. Ishii, H. Tatebe, H. Shiogama, A. Hasegawa, T. Toyoda, M. Mori, T. Suzuki, Y. Imada, T. Nozawa, K. Takata, T. Mochizuki, K. Ogochi, S. Emori, H. Hasumi, and M. Kimoto, 2011: MIROC4h—a new high-resolution atmosphere-ocean coupled general circulation model. *J. Meteor. Soc. Japan*, submitted.

Satoh, M., T. Matsuno, H. Tomita, H. Miura, T. Nasuno, and S. Iga, 2008: Nonhydrostatic icosahedral atmospheric model (NICAM) for global cloud resolving simulations. *J. Comput. Phys.*, **227**, 3486–3514.

Sen, O. L., Y. Wang, and B. Wang, 2004: Impact of Indochina deforestation on the East-Asian summer monsoon. *J. Climate*, **17**, 1366–1380.

Shimazu, Y., K. Nishi, T. Kamakura, M. Tahara, and T. Imataki, 2003: Meshed Climatological data. *Weather Service Bulletin*, **42**, 135–167 (in Japanese).

Skamarock, W. C., J. B. Klemp, J. Dudhia, D. O. Gill, D. M. Barker, M. G. Duda, X.-Y. Huang, W. Wang, and J. G. Powers, 2008: A Description of the Advanced Research WRF Version 3, *NCAR technical note*, NCAR/TN-475+STR.

Takayabu, I., H. Kato, K. Nishizawa, Y. N. Takayabu, Y. Sato, H. Sasaki, K. Kurihara, and A. Kitoh, 2007: Future Projections in Precipitation over Asia Simulated by Two RCMs Nested into MRI-CGCM2.2. *J. Meteor. Soc. Japan*, **85**, 511–519.

Tanaka, K., Y. Hagizawa, and T. Kojiri, 2008: Bias correc-

tion of RCM output considering frequency distribution. *Proc. of the 4th APHW Conference*, S4–14.

Taylor, K. E., 2001: Summarizing multiple aspects of model performance in a single diagram. *J. Geophys. Res.*, **106**, 7183–7192.

Walko, R. L., L. E. Band, J. Baron, T. G. F. Kittel, R. Lammers, T. J. Lee, D. Ojima, R. A. Pielke Sr, C. Taylor, C. Tague, C. J. Tremback, and P. J. Vidale, 2000: Coupled atmosphere-biophysicshydrology models for environmental modeling. *J. Appl. Meteor.*, **39**, 931–944.

Wang, S.-Y., R. R. Gillies, E. S. Takle, and W. J. Gutowski Jr., 2009: Evaluation of precipitation in the intermountain region as simulated by NARCCAP regional climate models. *Geophys. Res. Lett.*, **36**, L11704, doi:10.1029/2009GL037930.

Wang, Y. Q., O. L. Sen, and B. Wang, 2003: A highly resolved regional climate model (IPRC-RegCM) and its simulation of the 1998 severe precipitation event over China. Part I: Model description and verification of simulation. *J. Climate*, **16**, 1721–1738.

Yoshikane, T., F. Kimura, and S. Emori, 2001: Numerical Study on the Baiu Front Genesis by Heating Contrast between Land and Ocean. *J. Meteor. Soc. Japan*, **79**, 671–686.

Yoshikane, T., and F. Kimura, 2003: Formation mechanism of the simulated SPCZ and Baiu front using a regional climate model. *J. Atmos. Sci.*, **60**, 2612–2632.

Yukimoto, S., A. Noda, A. Kitoh, M. Hosaka, H. Yoshimura, T. Uchiyama, K. Shibata, O. Arakawa, and S. Kusunoki, 2006: Present-Day Climate and Climate Sensitivity in the Meteorological Research Institute Coupled GCM Version 2.3 (MRI-CGCM2.3). *J. Meteor. Soc. Japan*, **84**, 333–363.